Results of a 35-cm Xenon Ion Thruster Endurance Test*†

Shoji Kitamura
National Aerospace Laboratory of Japan
7-44-1 Jindaijihigashi-Machi, Chofu, Tokyo 182-8522 Japan
+81-422-40-3177
kitamura@nal.go.jp

Yukio Hayakawa and Katsuhiro Miyazaki
National Aerospace Laboratory of Japan
7-44-1 Jindaijihigashi-Machi, Chofu, Tokyo 182-8522 Japan

Ken'ichi Kajiwara
National Space Development Agency of Japan
2-1-1 Sengen, Tsukuba, Ibaraki 305-8505 Japan

Hideki Yoshida, Yuuko Yamamoto and Kouseki Akai
Toshiba Corporation
4-1 Ukishima-Cho, Kawasaki-Ku, Kawasaki, Kanagawa 210-0862 Japan

IEPC-01-083

An endurance test of a 35-cm xenon ion thruster aiming at 5,000-hour operation was conducted to evaluate the thruster grid life and to find out weak points in the thruster endurance. In April 2001, the total operation time reached 4,994 hours. The ion production cost was almost constant at about 120 W/A in the first half of the test, but increased to about 130 W/A in the second half. The highest temperature of the discharge chamber magnets was raised along with this increase. Thruster disassembly and inspection after the test revealed several eroded parts in the thruster. Grid mass measurements indicated that the screen grid mass was almost unchanged, but that the accelerator and decelerator grids suffered mass loss. Back-sputtering from the ion beam target lowered the accuracy in the measurement. However, rough estimation from the mass loss rate showed that the accelerator grid would endure longer than 20,000 hours.

Introduction

Ion propulsion systems provide an exhaust velocity, or specific impulse, more than an order of magnitude higher than that attainable with chemical thrusters. This can save large quantities of propellant. Though dry masses of ion propulsion systems are generally larger than those of chemical thrusters, the gains in mass savings are substantial, especially for missions requiring large velocity increments. They can be allotted for carrying more payloads, or more propellant to increase mission duration.

These gains can be used effectively both in auxiliary and primary ion propulsion systems. The most important application of auxiliary ion propulsion is north-south stationkeeping (NSSK) of geostationary satellites. Operational application of ion propulsion to NSSK has started in some countries. In Japan, ETS-6 and COMETS were launched in 1994 and 1998,

* Presented as Paper IEPC-01-083 at the 27th International Electric Propulsion Conference, Pasadena, CA, 15-19 October 2001.

respectively, which were equipped with ion thrusters for NSSK, though these thrusters were not used operationally but only experimentally because of the failures in inserting into the geostationary orbit [1]. As a next plan, however, ETS-8, equipped with ion thrusters, is scheduled for launch in 2004 [2]. In the United States, eight spacecraft using ion thruster systems were launched in 2000 [3]. In Europe, ion thrusters were flown on ARTEMIS in July 2001.

The next target for ion thruster application is primary propulsion. In the United States, the Deep Space-1 carried an ion thruster for primary propulsion [4]. In Japan, we started the research of 150-mN thrusters for future application to primary ion propulsion systems for orbit transfer and high-delta-V planetary missions.

We started with basic research on the thruster, and then moved to improving thruster performance [5] and [6]. Our current efforts are directed to improving thruster endurance. We already conducted a 1,000-hour test of a 35-cm xenon ion thruster, and found out some points for improving its endurance [7]. We then conducted a larger-scale endurance test of the improved thruster aiming at 5,000-hour operation [8]. The objectives of the test are to confirm the thruster operation at or near the target performance for 5,000 hours, and to estimate the survivability of the ion accelerating grids for a target lifetime of 30,000 hours. In this paper, we will describe the test apparatus, test conditions and procedures, and test results.

Apparatus and Procedure

Thruster

The thruster used for the endurance test is of ring-cusp type with a beam-exhausting diameter of 35 cm. It works with xenon as the propellant, and produces a nominal thrust of 150 mN at a specific impulse of 3,500 s and a total propellant flow rate of 3.27 A equivalent. The ion production cost is lower than 140 W/A at a discharge chamber propellant utilization efficiency of 90%. Here, the ion production cost is defined as the discharge voltage times the cathode emission current divided by the beam current. The thruster has a three-grid ion accelerating system. The grids are made of molybdenum and dished outward. Figures 1 and 2 show a cross-sectional view and a photograph of the thruster, respectively.

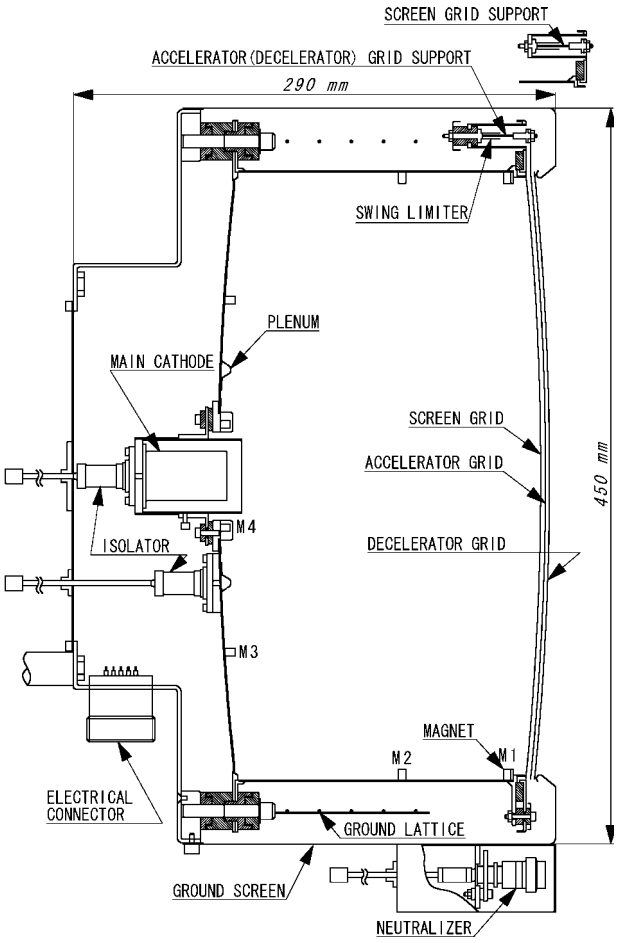

Figure 1 - Cross-sectional view of BBM-2 thruster.

Figure 2 - Photograph of BBM-2 thruster.

In the course of the research and development, thruster design and fabrication have been made several times to improve thruster performance. The thruster performance target was almost achieved in the breadboard model-1 (BBM-1) thruster. Table 1 gives a comparison of the target and achieved performance parameters. The BBM-1 thruster was already tested for 1,000 hours and some requirements were found out for improving thruster endurance [7].

The thruster used for the endurance test is the breadboard model-2 (BBM-2) thruster. Some improvements were incorporated in the BBM-1 thruster to make the BBM-2 thruster. The grids of the BBM-2 thruster were thickened to improve endurance. Table 2 shows the design parameters of the ion accelerating systems in both thrusters. The grids were fabricated using press welding. First, holes and outer shapes as in each of the grids were formed on 0.2-mm thick molybdenum plates by photochemical etching. Then, these original plates were piled and bonded to attain the required grid thickness. Each grid has 18,241 holes arranged in a hexagonal array.

The endurance test was started using the BBM-1 type main hollow cathode, which had been already used in the previous 1,000-hour test. Fabrication of BBM-2 type main cathodes was not finished in time. In the middle of the test, the main cathode assembly was replaced with a BBM-2 type cathode, which was designed to have much longer lifetime. However, the cathode insert was not replaced but used throughout the whole test period.

The BBM-2 thruster is identical with the BBM-1 thruster except for the ion accelerating system and main cathode. It is almost of cylindrical shape of 45 cm in diameter and 29 cm in length, and has an ion-beam exhausting diameter of 35 cm. The mass of the thruster is 12.5 kg.

The discharge chamber is 17.4 cm long, and has a regular polygonal cross-section of 24 sides with a circumscribed circle of 37-cm diameter. The walls of the discharge chamber are 1 mm thick and made of iron. A ring-cusp magnetic field is formed in the discharge chamber by four samarium/cobalt magnet rings; two are attached on the sidewall and the other two on the upstream wall.

Table 1. Target and Achieved Performance Parameters

Parameter	Target	Achieved
Thrust*, mN	150	150
Specific Impulse*†, s	3500	3518
Total Electric Power, kW	< 3.4	3.29
Propellant Flow Rate, mAeq.		
Discharge Chamber	3200	3200
Neutralizer	< 70	70
Total	< 3270	3270
Propellant Utilization†, %	90	90.0
Ion Production Cost§, W/A	< 140	104
Startup Time, min	< 10	13
Beam Supply Voltage, V	1000	1000
Beam Current, A	2.88	2.88
Accel. Grid Voltage, V	<500	300
Accel. Grid Current, mA	< 29	12.7
Decel. Grid Voltage, V	0	0
Decel. Grid Current, mA	< 29	7.0
Discharge Voltage, V	< 30	30.0
Discharge Current, A	< 16.4	12.9
Neut. Keeper Voltage, V	< 20	22.8
Neut. Keeper Current, A	< 1.2	1.0

* Not corrected for beam divergence and doubly charged ions.
† Neutralizer flow rate not included.
§ Discharge voltage x Emission current / Beam current.

Test Facilities

The endurance test was conducted using a vacuum facility with a chamber of 3 m in diameter and about 5 m in length. Figure 3 shows a schematic of the vacuum facility. This facility has a cryopanel at 50 K level to evacuate xenon gas at a pumping speed of about 200 m^3/s. The thruster is placed in the lock chamber while being accessed, and moved to the main chamber when it is operated. The typical pressure in the vacuum chamber is 7 to 9 x 10^{-6} Pa with no gas load, and 1 x 10^{-3} Pa with thruster operation, where these values are not corrected for xenon but readings for N_2.

During the test period, maintenance operations were conducted for the 50 K and 100 K helium coolers two times. During the first maintenance operation, the ion beam target was replaced because it had been damaged due to the ion beam impingement. The original

Table 2. Design Parameters of Ion Accelerating Systems

Type of Model	BBM-1			BBM-2		
Grid	Screen	Accelerator	Decelerator	Screen	Accelerator	Decelerator
Thickness, mm	0.4	0.6	0.6	0.6	0.8	0.6
Aperture Diameter, mm	2.2	1.4, 1.3, 1.2	1.8, 2.0	2.2	1.4, 1.3, 1.2	1.8, 2.0
Open Area Fraction, %	70	26	50	70	26	50
Curvature Radius, m	1.6	1.5	1.4	1.6	1.5	1.5
Grid Gap at Center, mm	1.4±0.1		1.3	1.4±0.1		0.8
Grid Gap at Periphery, mm	0.7±0.1		0.5	0.7±0.1		0.8

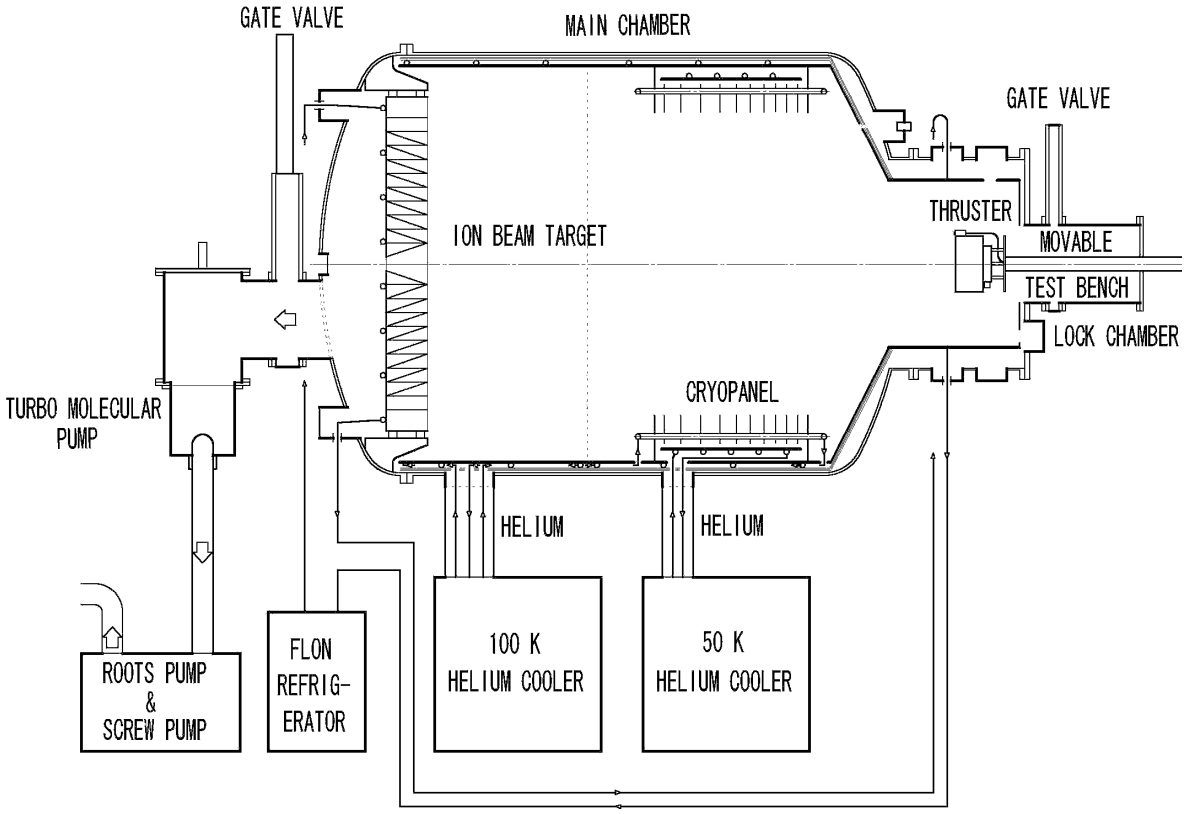

Figure 3 - Schematic view of test facility.

ion beam target was constructed with an aluminum lattice on an aluminum circular plate, and titanium plates were inserted oblique into most segments of the lattice. The new target had titanium chevrons arranged on a circular aluminum plate. After the replacement, however, back-sputtered efflux from the target was increased, and it caused more frequent high-voltage breakdown between the accelerator and decelerator

grids. The target was improved during the second maintenance period. The pointed ends of the chevrons were made much sharper to reduce the back-sputtered efflux. The chevron arrangement was changed so that the metal flakes on the target formed by the ion beam sputtering would fall off from the target more easily. The flakes left on the target could be the source to increase back-sputtering.

Test Conditions and Procedure

Test Conditions

The thruster was operated at a beam supply voltage of 1 kV, a beam current of 2.88 A, an accelerator grid voltage of –190 V, and a discharge voltage of 30 V. The accelerator grid voltage was made shallower from –300 V in the previous 1,000-hour test to reduce sputtering erosion of the accelerator grid by low energy ions, which were presumably created through charge-exchange and elastic collisions of beam ions with neutral xenon atoms.

The discharge current was adjusted manually to keep the constant beam current corresponding to a thrust of 150 mN. The discharge-chamber propellant flow rate was kept constant at 3.2 A equivalent. The ratio of propellant flow rates through the main cathode and main feed was adjusted to keep the discharge voltage at about 30 V.

The ion accelerating system was set up with the gaps shown in Table 2. At the beginning of the test, however, the gap between the accelerator and decelerator grids was increased to 0.9 mm to mitigate isolation breakdown between them. At 831-hour operation, it was recovered to the design value of 0.8 mm.

Test Procedure

Ahead of the endurance test, a preparatory thruster operation was conducted for about 200 hours to stabilize thruster performance. In the endurance test, the thruster was operated as continuously as possible. However, the operation had to be interrupted many times, mainly for reasons related to the vacuum facility.

In the endurance test, thruster performance parameters were monitored, and temperatures were measured at several parts of the thruster. Grid mass measurements were conducted just before starting the test, in the middle, and after the end of the test. Back-sputtered efflux from the ion beam target was measured using a quartz crystal microbalance just after each of the replacement and improvement of the ion beam target. After the test, the thruster was disassembled and inspected using a microscope and a borescope.

Results and Discussion

Chronology

The test was started on September 10, 1999 and finished on April 1, 2001. The accumulated thrusting time reached 4,994 hours and 14 minutes. Though the thruster operation could be continued longer, the test was stopped for thruster inspection and evaluation. Table 3 summarizes the chronology for main events along with the accumulated thrusting time. Figure 4 shows the increase in the thrusting time along with the elapsed time. The two longest horizontal segments of the plot in Figure 4 correspond to the periods for the maintenance operations of the helium coolers and the target replacement and improvement. The accumulated thrusting time was 37% of the total elapsed time, and was 64% of the elapsed time excluding the periods for the maintenance operations.

Interruptions of Thruster Operation

During the test period, the vacuum facility was stopped for several reasons. The most frequent among them was chamber pressure increase due to temperature rise of the cryopanel. Contamination was brought about on the cryopanel surface during thruster operation, and it increased the thermal absorption coefficient of the cryopanel surface. This caused increase in thermal input to the cryopanel, and its temperature was raised because the helium cooler for the cryopanel has only a marginal cooling capability. In these cases, vacuum system maintenance was conducted. The cryopanel was cleaned up to remove the contaminant, and also the ion beam target was cleaned up to remove metal flakes formed by the ion beam sputtering.

Table 3. Chronology of Endurance Test

Date month/day/year	Thrusting Time h:min	Event
09/10/99	00:00	Test started
09/22/99	274:50	Vacuum system maintenance
10/08/99	533:49	Vacuum system maintenance
11/01/99	830:54	Vacuum system maintenance
11/19/99	1,049:02	Vacuum system maintenance
12/10/99	1,355:44	Vacuum system maintenance
12/26/99	1,606:13	Vacuum system maintenance
01/23/00	2,065:10	Vacuum system maintenance
02/12/00	2,447:56	Vacuum system maintenance
02/19/00	2,509:39	Grid-mass measurement Main cathode replaced
02/22/00	2,536:13	Vacuum system maintenance
03/03/00	2,659:51	Ion beam target replaced
05/29/00	2,882:07	Thruster cleaned up Cathode position changed
06/02/00	2,970:36	Thruster damaged from improper handling
06/23/00	3,288:52	Thruster cleaned up Cathode position changed
06/27/00	3,310:30	Vacuum system maintenance
07/14/00	3,538:27	Vacuum system maintenance
08/11/00	3,885:47	Vacuum system maintenance
09/01/00	4,135:14	Ion beam target improved
04/01/01	4,994:14	End of test

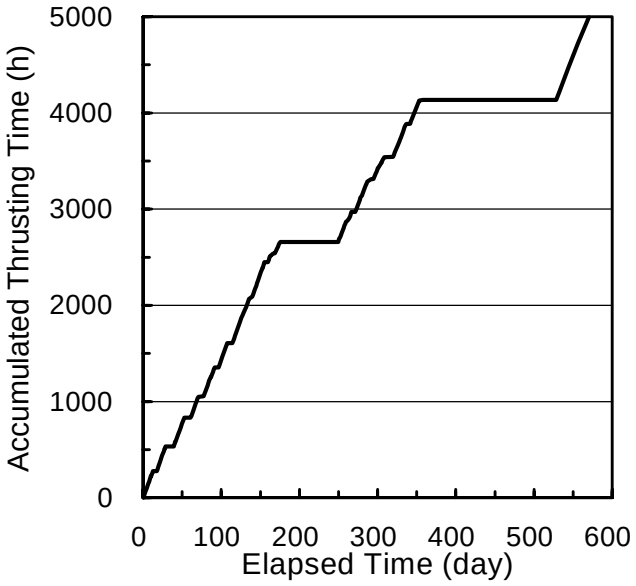

Figure 4 - Increase in thrusting time with elapsed time.

Table 4. Test Interruptions and Causes

Test Interruption		Count
Thruster related	Main discharge extinction	20
	Excessive accel grid current	12
	Neutralizer ignition failure	1
	Subtotal	33
Facility related	Vacuum degradation	25
	Xenon gas shortage	1
	Power supply failure	1
	Subtotal	27
Intentional	Xenon bottle exchange	10
	Power and water stoppage	4
	Power supply inspection / repair	4
	Grid mass measurement	1
	Year 2K problem counteraction	1
	Subtotal	20
Total		80

The thruster operation was interrupted more frequently, and the interruptions counted 80 in total, including the interruptions due to the facility problems above-mentioned. Table 4 summarizes these interruptions and causes for them.

Some of the test interruptions were caused by thruster-related problems. The main discharge extinctions were triggered by short between the accelerator and decelerator grids. However, extinctions in the main cathode discharge have ceased since some modifications were made in the starting sequence of the high-voltage application. The accelerator grid current became excessive when whisker-like metal flakes bridged between the accelerator and decelerator grids. The neutralizer ignition failure occurred once, and presumably it was caused by some foreign material which plugged the neutralizer orifice.

The test facility had problems resulting in test interruptions. The vacuum degradation was judged by the vacuum chamber pressure. The thruster operation was stopped automatically or manually when the chamber pressure exceeded about 1.5 to 3 x 10^{-3} Pa. There were scheduled power stoppage three times and water stoppage once during the test period. The test was interrupted in the period from the end of 1999 to the beginning of 2000 to avoid accidental Y2K problems.

Thruster Inspection

Metal Flakes
The grid system was removed from the thruster and inspection was conducted two times, in the middle of the test (2,509 h 39 min) and at the end of the test (4994 h 14 min). Flakes were found at the iron ring which was placed adjacent to the magnet ring M1 for absorbing magnetic flux and at the ring for supporting the accelerator grid. A small amount of flakes were found at some of the other parts of the thruster. No flakes were found on the magnet rings, the inside surface of the discharge-chamber sidewall, the main cathode keeper, and the edge of the main cathode support cylinder.

Main Cathode
The total operation time of the main cathode insert counted about 6,200 hours, consisting of 1,000 hours in the pervious long test, 200 hours in the preparatory test and 5,000 hours in this test. The other parts of the main cathode were used for about 2,500 hours in the second half of this test.

The main cathode was disassembled for inspection after the test. The insert showed no considerable changes in appearance. The orifice plate had an eroded region around the center of the downstream surface. No damages were found in the heater part on the cathode tube. In the cathode keeper, contamination was so slight that insulation problems would not occur. The cathode support cylinder was eroded at its downstream edge.

Other Parts
The outside surfaces of the discharge chamber are coated with alumina to facilitate thermal radiation cooling. Contamination of these surfaces was slight on the upstream wall, but considerable on the sidewall.

A crack was found on the magnet cover, as shown in Figure 5, which was installed over the magnet ring M4 for discharge current bypassing. The crack was located along the cusp lines on the magnet ring. A part of the crack penetrated the entire thickness of the cover made of molybdenum.

Figure 5 - Photograph of cracked magnet cover.

Thruster Performance

In the endurance test, the thruster was operated stably nearly at the target thrust and specific impulse of 150 mN and 3,500 s, respectively. The propellant flow rate and total electric power satisfied the respective targets less than or equal to 3.27 A equivalent and 3.4 kW.

Figures 6 through 10 show the time variations in the ion production cost, discharge-chamber propellant utilization efficiency, discharge current, discharge voltage, and accelerator grid current, respectively. Each data point in these plots was obtained while the thruster was being operated stably with a certain stabilizing time after starting each operation. In the latter half of the test period, however, data scattering was noticeable. This is because it was often difficult to achieve stable thruster operation due to frequent arcing between the accelerator and decelerator grids.

The ion production cost in the latter half period was about 10 W/A larger than that in the first half. The replacement of the main cathode is the most probable reason for this increase. The most noticeable increase occurred at about 2,500 hours, when the main cathode was exchanged. Increase in the accelerator-grid hole diameters would be also a possible reason for the increase in the ion production cost; the discharge-chamber propellant utilization efficiency was kept constant. If this was the case, the increase in the ion production cost should have been approximately in accordance with mass loss in the grid, or almost with the thrusting time. Moreover, rough estimation

suggested that the 10 W/A-increase in ion production cost would be too large to occur due to grid hole enlargement in this test. In spite of this increase, the ion production cost was kept within the target through the test.

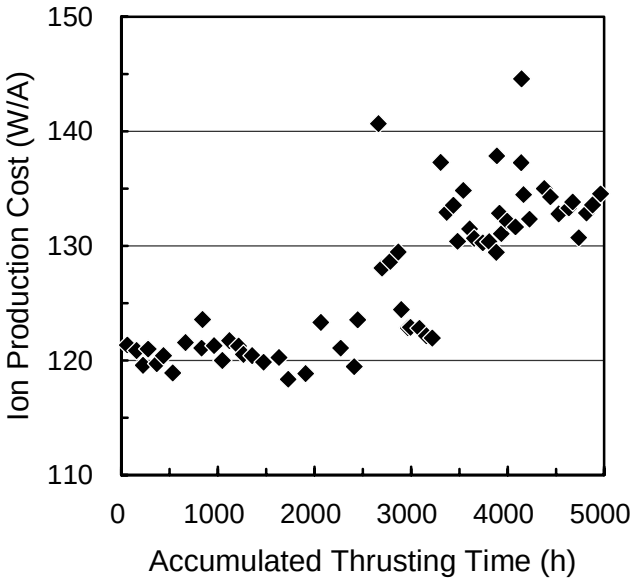

Figure 6 - Variations in ion production cost.

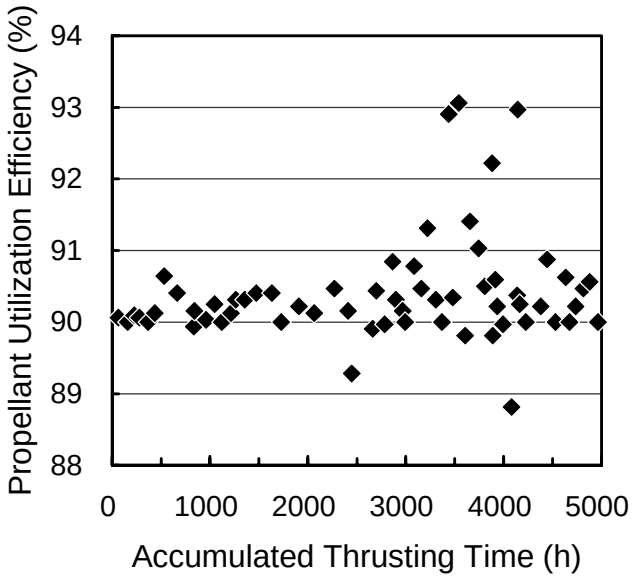

Figure 7 - Variations in discharge-chamber propellant utilization efficiency.

The discharge-chamber propellant utilization efficiency was kept near 90% by adjusting the discharge current. The discharge voltage was kept at about 30 V by changing the propellant flow rate ratio of the main cathode and main feed. The accelerator grid current

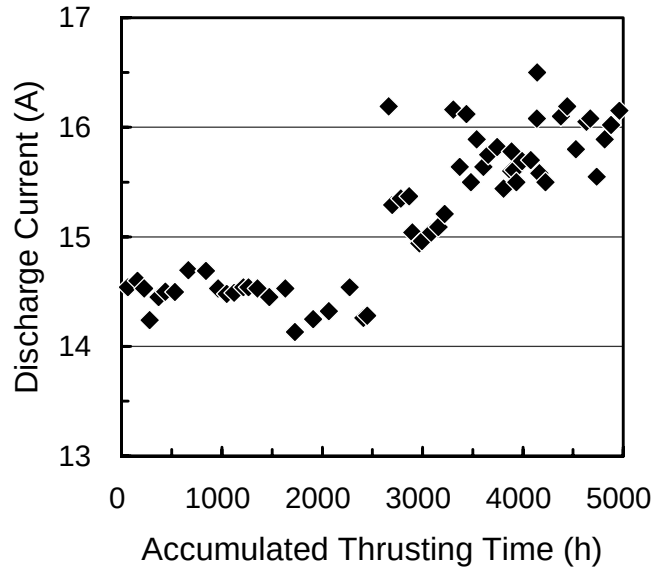

Figure 8 - Variations in discharge current.

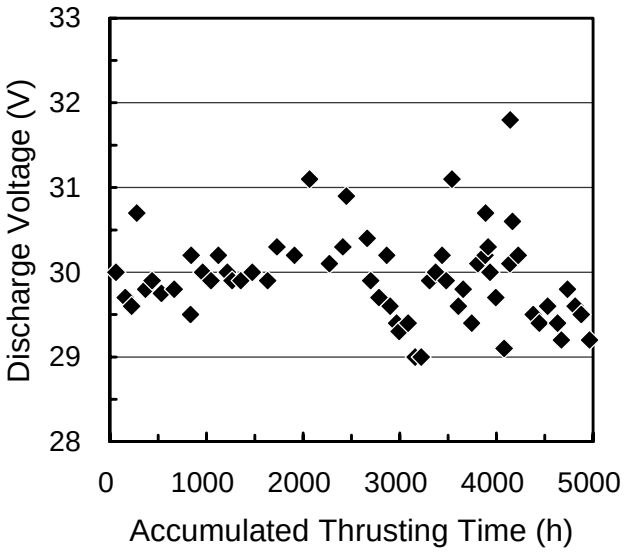

Figure 9 - Variations in discharge voltage.

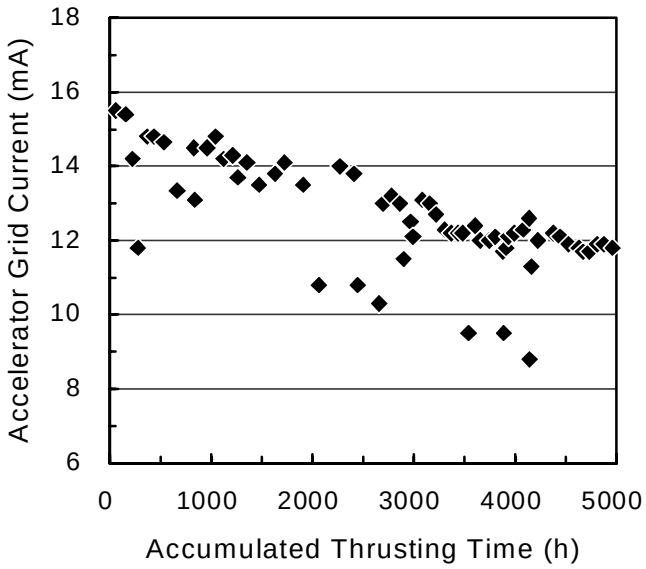

Figure 10 - Variations in accelerator grid current.

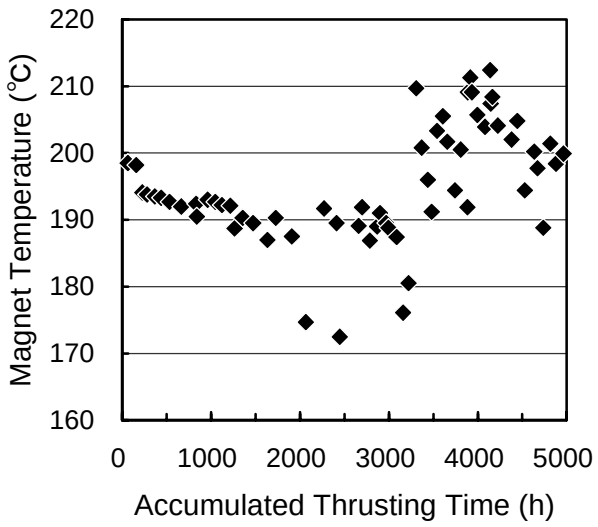

Figure 12 - Temperature variations of magnet ring M4.

Table 5. Magnet Temperatures

Magnet	Accumulated thrusting time, h		
	2	2,510	4,959
M1, EC	142±21	138±21	129±22
M2, EC	161±13	156±13	149±14
M3, EC	179±13	173±13	185±14
M4, EC	202	190	207

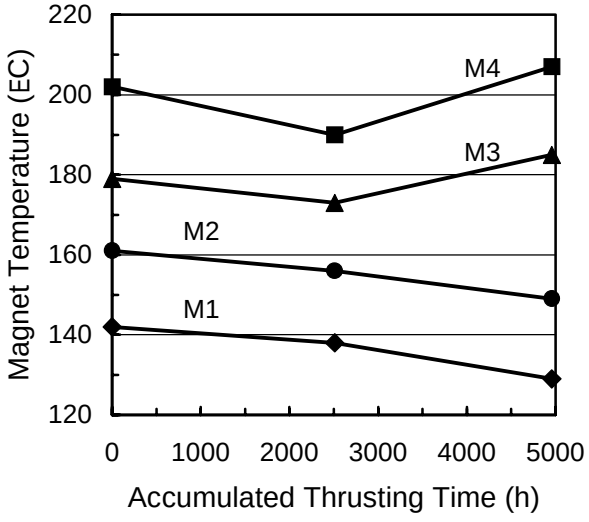

Figure 11 - Temperatures at discharge-chamber magnet rings.

was approximately 0.4–0.5% of the beam current. It tended to decrease with thrusting time because of the enlargement of the accelerator grid holes with time. The decrease in the accelerator grid current had a tendency to level off toward the end of the test.

Magnet Temperatures

Temperatures of several parts of the thruster were measured in the test. They were leveled off in about two hours after starting each operation, and kept almost constant afterwards. Temperatures of the magnet rings were estimated from these data. Temperature rises of the magnet rings due to the discharge current going through the magnets were considered in the estimation for the magnet rings M1 through M3. Results are shown in Table 5, and plotted in Figure 11. Figure 12 shows detailed time variations in the temperature of the magnet ring M4.

The temperatures of all the magnet rings were lowered with time in the first half of the test, and those of the magnet rings M1 and M2 continued to be lowered even in the latter half, for which the ion production cost was increased. This suggests that the thermal radiation from the thruster was increased with time because the discharge power of the thruster was unchanged or increased. There are two presumable

reasons for facilitating the thermal radiation. One is enlargement of the grid hole diameters, and the other is increase in the thermal radiation from the discharge-chamber walls. Enlargement of the hole diameters in the accelerator grid is actually supported by its mass loss. It is possible that the thermal radiation from the discharge-chamber walls was increased by contamination, though it depends on kinds of the contaminants.

The temperatures of the magnet rings M3 and M4 were raised with time in the latter half of the test. In this period, the ion production cost was increased, and this gives a reasonable explanation for these temperature rises. Changes in the discharge current distribution among the magnet rings are suggested by the fact that temperatures were raised only at the magnet rings M3 and M4 out of the four. This is consistent with the cracking found in the magnet cover, where the discharge current was probably concentrated to some extent. There are two presumable reasons for this current concentration; degradation in the magnet ring M4, and the eroded downstream edge of the main cathode support cylinder.

The temperature of the magnet ring M4 exceeded 200 EC after about 3,300 hours, and the magnet cover for the magnet ring M4 suffered cracking. These have caused concern about magnet degradation. However, measurements on the magnet degradation have not been conducted yet, but only a simple check was done. A piece of iron attracted by the magnets was pulled away by hand. No noticeable changes were found in the pulling forces compared with normal magnets. Efforts to keep the low levels of ion production cost would be necessary to prevent possible magnet degradation in much longer operation.

Ion Accelerating System

Results of the grid mass measurements are shown in Table 6, and plotted in Figure 13. For the decelerator grid, an additional measurement was conducted at 831 hours, when the grid spacing from the accelerator grid was changed. The accelerator grid had the largest mass loss rate, and is critical to the life of the grid system.

Table 6. Mass Changes of Grids

Time h:min	Screen grid g	Accel. grid g	Decel.grid g
0:0	285.880	702.90	383.314
	(0)	(0)	(0)
830:54	-	-	376.143
			(-7.171)
2509:39	287.526	689.20	375.238
	(+1.646)	(-13.70)	(-8.076)
4994:14	286.977	670.75	376.339
	(+1.097)	670.45*	372.293*
		(-32.45)	(-11.021)

*After metal deposition on the surface was peeled off mechanically as thoroughly as possible.

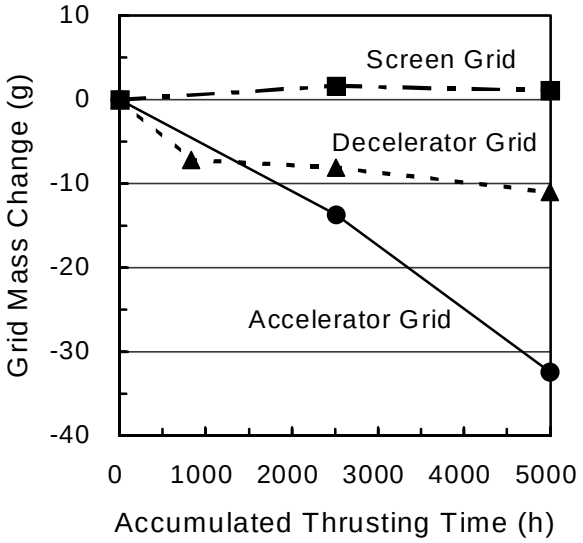

Figure 13 - Grid mass changes with time.

To supplement the grid mass measurements, back-sputtered efflux from the ion beam target to the thruster was measured using the quartz crystal microbalance placed near the thruster. The measurements were conducted two times, after each of the ion target replacement and improvement. Measured deposition rates per unit ion beam current and time were 3.17 nm/(Ah) and 2.44 nm/(Ah), respectively. Here the deposited material was assumed to be titanium, which composes most of the target surface sputtered by the ion beam.

Screen Grid
The mass change rate of the screen grid was +0.656 mg/h (gain) in the first half of the test, -0.221 mg/h (loss) in the second half, and +0.220 mg/h (gain) on the average. No serious problems were found as far as the mass changes were concerned.

In the microscope inspection, it was found that the upstream surface of the screen grid became rough in the center region. The borescope inspection showed that the edge areas surrounding the grid holes were raised from the original upstream surface level in the center region, as shown in Figure 14. If these raises continue to develop, it will increase the effective grid thickness, and may affect the ion production cost.

Accelerator Grid
The mass change rate of the accelerator grid was -5.46 mg/h (loss) in the first half of the test, -7.55 mg/h (loss) in the second half, and –6.50 mg/h (loss) on the average. Assuming that enlargement of the grid hole diameters causes all the grid mass loss, estimation was made on the grid lifetime. Accelerator grid lifetime was defined as the time when its hole diameters become enlarged up to the hole diameter of the original decelerator grid. Then, the lifetime was estimated at about 25,000 hours. Unequal enlargement among the holes would make the lifetime shorter. The tendency of decreasing accelerator grid current would make the mass loss rate smaller, and suggest longer lifetime.

The mass loss measurement of the accelerator grid may be affected by the back-sputtering from the target and sputtered material from the decelerator. The lifetime estimation above should be treated in the level of accuracy neglecting these effects.

The deposition rate of the back-sputtered material on the accelerator grid was estimated from the deposition rate on the quartz crystal microbalance to be 0.96 and 0.74 mg/h for the two measurements, respectively. Here, the deposition on the accelerator grid was assumed to come through the decelerator grid holes, and the grid open area fractions were assumed unchanged from their respective original values. The estimated deposition rate is not negligible, but approximately one-order-of-magnitude smaller than the mass loss rate.

The effect of the sputtered material from the decelerator is not large after 831 hours. The mass loss rate of the decelerator grid was 1.19 mg/h in the second half of the test. It is much smaller than that of the accelerator grid, and, moreover, the deposition on the accelerator grid coming from the decelerator grid would be a fraction of the mass loss of the decelerator grid.

Decelerator Grid
In the decelerator grid, sever enlargement of the grid holes was found in the periphery region, and some of the grid web was totally eroded, as shown in Figure 15. This was attributed mainly to the unconverged high-energy ions. Most of the erosion occurred while the grid spacing to the accelerator grid was set larger than the design value. After it was recovered at 831 hours, the mass loss rate became much smaller, as shown in Figure 13. After that, however, the mass loss still continued, and thus the lost or thinned portion of the grid web may cause structural problems of the decelerator grid. Counteractions are required such as making the corresponding screen grid holes smaller or partly closed.

Conclusions

The thruster was operated for 4,994 hours in total, and it could be operated longer. The thruster performance was kept at the targets of 150 mN thrust, 3,500 s specific impulse and under 140 W/A ion production cost at 90% discharge-chamber propellant efficiency. The estimated grid lifetime is longer than 20,000 hours, though it did not reach the target of 30,000 hours yet. The BBM-2 main cathode was operated for 2,485 hours.

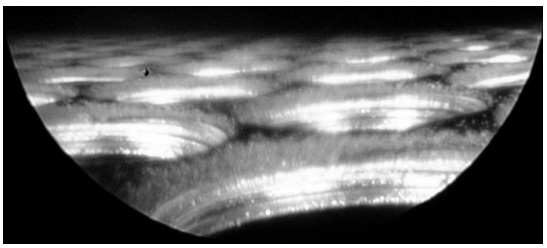

Figure 14 - Screen grid holes in center region.

References

[1] Kimiya Komurasaki, Yoshihiro Arakawa and Haruki Takegahara, “An Overview of Electric and Advanced Propulsion Activities in Japan,” *Proceedings of 3rd International Conference on Spacecraft Propulsion,* October 10-13, 2000.

[2] Toshiyuki Ozaki et al., “Development Status of Xenon Ion Thruster for ETS-8,” ISTS-2000-b-10, May 2000.

[3] R. Joseph Cassady, “Overview of Major U.S. Industrial Programs in Electric Propulsion,” AIAA-2001-3226, July 2001.

[4] John Dunning, “NASA’s Electric Propulsion Program: Technology Investments for the New Millennium,” AIAA-2001-3224, July 2001.

[5] Hideki Yoshida et al., “Performance Characteristics of a 35-cm Diameter Xenon Ion Thruster,” AIAA-96-2714, July 1996.

[6] Shoji Kitamura et al., “Research and Development Status of 150-mN Xenon Ion Thrusters,” IAF-00-S.4.06, October 2000.

[7] Shoji Kitamura et al., “1000-hour Test of a 35-cm Diameter Xenon Ion Thruster,” IEPC-99-142, October 1999.

[8] Yukio Hayakawa et al., “5000-hour Endurance Test of a 35-cm Xenon Ion Thruster,” AIAA-2001-3492, July 2001.

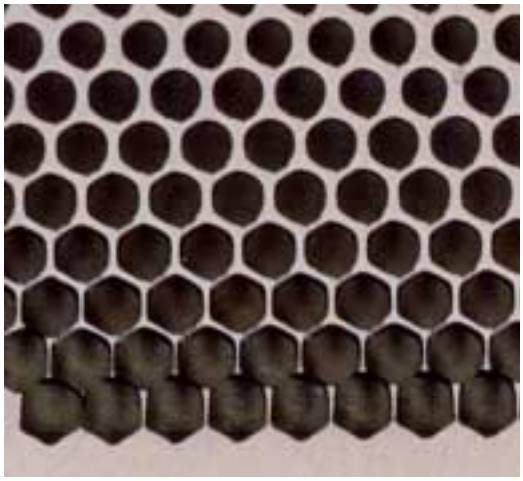

Figure 15 - Decelerator grid holes in periphery region.